

Published in final edited form as:

*Brain Res.* 2013 November 13; 1538: . doi:10.1016/j.brainres.2013.09.028.

## Postnatal development of glycine receptor subunits $\alpha 1$ , $\alpha 2$ , $\alpha 3$ , and $\beta$ immunoreactivity in multiple brain stem respiratory-related nuclear groups of the rat

QIULI LIU and MARGARET T.T. WONG-RILEY

Department of Cell Biology, Neurobiology and Anatomy, Medical College of Wisconsin, Milwaukee, Wisconsin, 53226, USA

### Abstract

The respiratory system is immature at birth and significant development occurs postnatally. A critical period of respiratory development occurs in rats around postnatal days 12-13, when enhanced inhibition dominates over suppressed excitation. The mechanisms underlying the heightened inhibition are not fully understood. The present study tested our hypothesis that the inhibition is marked by a switch in glycine receptor subunits from neonatal to adult form around the critical period. An in-depth immunohistochemical and single neuron optical densitometric study was undertaken on four respiratory-related nuclear groups (the pre-Bötzing complex, nucleus ambiguus, hypoglossal nucleus, and ventrolateral subnucleus of solitary tract nucleus), and a non-respiratory cuneate nucleus in P2-21 rats. Our data revealed that in the respiratory-related nuclear groups: (1) the expressions of GlyR  $\alpha 2$  and GlyR  $\alpha 3$  were relatively high at P2, but declined after 1-1½ weeks to their lowest levels at P21; (2) the expression of GlyR  $\alpha 1$  increased with age and reached significance at P12; and (3) the expression of GlyR  $\beta$  rose from P2 to P12 followed by a slight decline until P21. No distinct increase in GlyR  $\alpha 1$  at P12 was noted in the cuneate nucleus. Thus, there is a switch in dominance of expression from neonatal GlyR  $\alpha 2/3$  to the adult GlyR  $\alpha 1$  and a heightened expression of GlyR  $\beta$  around the critical period in all respiratory-related nuclear groups, thereby supporting enhanced inhibition at that time. The rise in the expression of GlyR  $\beta$  around P12 indicates that it plays an important role in forming the mature heteropentameric glycine receptors in these brain stem nuclear groups.

### Keywords

critical period; cuneate nucleus; hypoglossal nucleus; nucleus ambiguus; pre-Bötzing complex; ventrolateral subnucleus of solitary tract nucleus

---

© 2013 Elsevier B.V. All rights reserved.

**Corresponding Author:** Margaret T.T. Wong-Riley, Ph.D. Department of Cell Biology, Neurobiology, and Anatomy, Medical College of Wisconsin, 8701 Watertown Plank Road Milwaukee, WI 53226 Tel.: 1-414-955-8467 Fax: 1-414-955-6517 mwr@mcw.edu.

**Publisher's Disclaimer:** This is a PDF file of an unedited manuscript that has been accepted for publication. As a service to our customers we are providing this early version of the manuscript. The manuscript will undergo copyediting, typesetting, and review of the resulting proof before it is published in its final citable form. Please note that during the production process errors may be discovered which could affect the content, and all legal disclaimers that apply to the journal pertain.

Conflict of interest

Both authors declare no competing financial interests.

## 1. Introduction

In rats, a critical period in respiratory network development exists around postnatal days (P) 12-13, when a striking and transient imbalance between enhanced expression of inhibitory neurochemicals and suppressed expression of excitatory neurochemicals occurs in multiple respiratory-related brain stem nuclear groups (Liu and Wong-Riley, 2002, 2005; Wong-Riley and Liu, 2005, 2008; Wong-Riley et al., 2013). Such an imbalance is also demonstrable electrophysiologically at the synaptic level (Gao et al., 2011). During this narrow window, there is an apparent switch in GABA<sub>A</sub> receptor subunits from the neonatal  $\alpha 3$  to the adult  $\alpha 1$  form (Liu and Wong-Riley, 2004, 2006), and a switch from the neonatal Cl<sup>-</sup>-intruder Na<sup>+</sup>-K<sup>+</sup>-2Cl<sup>-</sup> co-transporter 1 (NKCC1) to the adult Cl<sup>-</sup>-extruder K<sup>+</sup>-Cl<sup>-</sup> co-transporter 2 (KCC2) (Liu and Wong-Riley, 2012), in multiple brain stem respiratory-related nuclear groups. Moreover, the ventilatory and metabolic responses to hypoxia are at their weakest at this time (Liu et al., 2006, 2009).

The enhanced inhibition during the critical period is likely to be mediated by two major inhibitory neurotransmitters, GABA and glycine, and their receptors. Significantly, in the respiratory-related hypoglossal nucleus (XII), a switch in dominance from GABAergic to glycinergic synaptic transmission is evident at the beginning of the second postnatal week, being most prominent during the critical period (Gao et al., 2011). At this time, the expression of glycinergic receptors is significantly increased in multiple respiratory-related nuclear groups of the brain stem (Liu and Wong-Riley, 2002, 2005).

Glycine receptors (GlyR) are pentameric ligand-gated Cl<sup>-</sup> channels made up of  $\alpha 1$ ,  $\alpha 2$ , or  $\alpha 3$  with or without  $\beta$  subunits (reviewed in Kuhse et al., 1991; Dutertre et al., 2012).  $\alpha 4$  subunit is reported thus far mainly in the retina (Heinze et al., 2007). Glycine receptors undergo subunit changes during development in different parts of the nervous system (Malosio et al., 1991; Aroeira et al., 2011; Jonsson et al., 2012). However, the distribution and developmental patterns of the various GlyR subunits are virtually unknown within the brain stem respiratory system.

The present study was undertaken to test our hypothesis that the heightened inhibition during the critical period is marked by a switch in glycine receptor subunits from the neonatal to the adult form. We conducted an in-depth immunohistochemical and single neuron optical densitometric analysis of GlyR  $\alpha 1$ ,  $\alpha 2$ ,  $\alpha 3$ , and  $\alpha 4$  subunits in four respiratory-related nuclear groups and one nonrespiratory nucleus of P2–21 rats. The respiratory-related nuclear groups are the pre-Bötzing complex (PBC, a presumed center or kernel for respiratory rhythmogenesis; Smith et al., 1991, 2000; Rekling and Feldman, 1998); nucleus ambiguus (Amb, which receives input from the central respiratory network and innervates airway muscles of the pharynx and larynx to maintain upper airway patency; Jordan, 2001); hypoglossal nucleus (XII, which innervates the tongue and pharyngeal muscles important for maintaining upper airway patency during breathing; Lowe, 1980; Jordan, 2001); and the ventrolateral subnucleus of the solitary tract nucleus (NTS<sub>VL</sub>, which receives direct projections from pulmonary stretch receptor afferents of the vagus, the superior laryngeal nerves, as well as peripheral chemoafferents; contains inspiratory neurons and is part of the dorsal respiratory group known to project directly or indirectly via the pontine respiratory group to the ventral respiratory column; McCrimmon et al., 1987; Smith et al., 1989, 2013; Ellenberger and Feldman, 1990; Holtman et al., 1990; Finley and Katz, 1992; Bonham, 1995; Subramanian et al., 2007; Yokota et al., 2008; Wong-Riley et al., 2013). The non-respiratory cuneate nucleus (CN) is a relay in the somatosensory system with no known respiratory function, and it served as an internal control.

## 2. Results

### 2.1. GlyR $\alpha$ 1-immunoreactive (-ir) neurons in the brain stem nuclear groups

GlyR 1-ir was clearly visible in subpopulations of neurons in all five brain stem nuclear groups examined (Fig. 1A, B). Immunoreaction product was present in cell bodies and proximal dendrites of labeled neurons as well as in the neuropil (including dendritic processes). The plasma membrane of labeled neurons showed clear immunoreaction product (see insets in Fig. 1). The sizes of GlyR 1-ir neurons increased with age and reached a level at P11-P12 approximately 85-95% of that at P21 (Fig. 1). Control sections had no specific immunoreactivity above background (data not shown). One-way ANOVA indicated significant differences ( $P < 0.01$ ) in GlyR 1-ir among the ages in the PBC, Amb, XII, and NTS<sub>VL</sub>, but not in the CN. Tukey's Studentized range test that compared one age group with its adjacent younger tested age group revealed a significant rise at P12 for PBC, Amb, and XII ( $P < 0.01 - P < 0.001$ , as compared to the values at P11), but not for CN (Fig. 2).

**2.1.1. GlyR $\alpha$ 1-immunoreactive neurons in the PBC**—GlyR 1-ir was observed in ~ 45% - 60% of the PBC neurons. They were multipolar, granular, or fusiform in shape and small or medium in size (Fig. 1C-F). The size of small neurons ranged from 5 to 8  $\mu$ m in diameter at P2 to 7-9  $\mu$ m at P21, and medium-sized neurons ranged from 9.5 - 14  $\mu$ m at P2 to 12 - 20.5  $\mu$ m at P21. The expression of GlyR 1 increased gradually from P2 to P7 ( $P < 0.05$  for Tukey's test between P2 and P7), but significantly from P11 to P12 ( $P < 0.001$ ), followed by a plateau until P21 (Fig. 2A). P12 was the only time point in the first 3 postnatal weeks when a day-to-day significance was found. Tukey's test also revealed that the values at P12, P13, and P14 were significantly higher than those of each tested day from P2 to P11 ( $P < 0.05 - P < 0.001$ ), and the values at P17 and P21 were significantly higher than those of P2 and P3 ( $P < 0.05 - P < 0.001$ ).

**2.1.2. GlyR $\alpha$ 1-immunoreactive neurons in the Amb**—About 50% - 65% of Amb neurons demonstrated GlyR 1-ir. These neurons were multipolar or oval in shape and mainly medium or small in size (Fig. 1G-J). The size of small neurons ranged from 6 to 8.5  $\mu$ m in diameter at P2 to 7 - 11  $\mu$ m at P21, and medium-sized neurons ranged from 11 - 15  $\mu$ m at P2 to 16.5-21  $\mu$ m at P21. Occasionally, a few large labeled neurons (24 - 28  $\mu$ m in diameter) were observed at P21. GlyR 1 immunoreactivity exhibited a trend similar to that of the PBC, with a significant increase at P12 ( $P < 0.01$ ) (Fig. 2B). Tukey's test also yielded significant differences between values at P12-13 and those of each individual days from P2 to P11 ( $P < 0.05 - P < 0.01$ ), except for P7.

**2.1.3. GlyR $\alpha$ 1-immunoreactive neurons in the XII**—GlyR 1-ir was present in ~ 80% - 90% of XII neurons. They were multipolar, oval, or fusiform in shape and mainly medium or large in size (Fig. 1K-N). Medium-sized neurons ranged from 11 to 15  $\mu$ m in diameter at P2 to 14 - 20.5  $\mu$ m at P21, and large neurons ranged from 17 - 19.5  $\mu$ m at P2 to 24 - 28.5  $\mu$ m at P21. The developmental trend of GlyR 1-ir was comparable to those of the PBC and Amb, with a gradual increase from P2 to P7 ( $P < 0.01$  for Tukey's test between the two time points) and a significant rise at P12 ( $P < 0.001$ ) (Fig. 2C). Tukey's test also showed that the value at each individual days from P12 to P21 was significantly higher than those of each tested day from P2 to P11 ( $P < 0.01 - P < 0.001$ ), except for P7.

**2.1.4. GlyR $\alpha$ 1-immunoreactive neurons in the NTS<sub>VL</sub>**—GlyR 1-ir was observed in about 35% - 50% of the NTS<sub>VL</sub> neurons. They were multipolar, granular, oval, or fusiform in shape and mainly small in size (Fig. 1O-R). The small neurons ranged from 5 - 8  $\mu$ m in diameter at P2 to 7 - 11.5  $\mu$ m at P21. Occasionally, a few of medium-sized neurons (14.5 - 19.5  $\mu$ m in diameter) were observed at P17-21. The expression of GlyR 1 increased

gradually from P2 to P10 ( $P < 0.05$  for Tukey's test between the two time points), followed by a significant rise at P12 ( $P < 0.001$ ) and a gradual decline at P13-14, then plateaued until P21 (Fig. 2D). Tukey's test also yielded significance in values between each individual days at P12, P13, P21 and each day from P2 to P11 ( $P < 0.05 - P < 0.001$ , except for a lack of significance between P10 and P21), between P2 or P3 and P14 or P17 ( $P < 0.05 - P < 0.01$ ), as well as between P12 and P14, P17, or P21 ( $P < 0.05 - P < 0.01$ ).

**2.1.5. GlyR $\alpha$ 1-immunoreactive neurons in the CN**—About 30% - 50% of neurons in the CN demonstrated GlyR 1-ir (Fig. 1S-V). These labeled neurons were oval, multipolar, or granular in shape and mainly small in size. Small neurons ranged from 5 - 7.5  $\mu\text{m}$  in diameter at P2 to 6 - 12.5  $\mu\text{m}$  at P21, and medium-sized labeled neurons ranged from 8.5 - 10  $\mu\text{m}$  at P2 to 14 - 19  $\mu\text{m}$  at P21. The expression of GlyR 1 showed a much gentler rise from P2 to P21 (Fig. 2E). However, Tukey's test did not yield significant differences between any two age groups.

Two-way ANOVA indicated significant differences in GlyR 1 expression among the five nuclear groups ( $P < 0.01$ ). Subsequent Tukey's tests revealed that the values were significantly higher in XII than in CN between P12 and P17 ( $P < 0.05 - P < 0.01$ ). They were also higher in XII than in Amb at P12 ( $P < 0.05$ ).

## 2.2. GlyR $\alpha$ 2-immunoreactive neurons in the brain stem nuclear groups

In general, GlyR 2-ir product was clearly visible in subpopulations of neurons in each of the brain stem nuclear group examined (Fig. 3A, B). Labeling was present in cell bodies and proximal dendrites of neurons as well as in the neuropil. Labeling could also be observed along the plasma membrane (see insets in Fig. 3). Developmental changes in sizes and shapes of GlyR 2-ir neurons were comparable to those of GlyR 1-ir neurons, and will not be described in detail below. Control sections demonstrated no specific immunoreactive product above background (data not shown). One-way ANOVA indicated significant differences ( $P < 0.01$ ) in GlyR 2-ir among the ages in the PBC, Amb, XII, and NTS<sub>VL</sub>, but Tukey's test failed to yield significant differences between any two adjacent tested age groups. Significant differences between non-adjacent age groups are detailed below.

**2.2.1. GlyR $\alpha$ 2-immunoreactive neurons in the PBC**—GlyR 2-ir was observed in ~ 45% - 55% of the PBC neurons (Fig. 3C-F). The expression of GlyR 2 was relatively high from P2 to P7, followed by a gradual decline until P21 (Fig. 4A). Although no significant differences were found between any two adjacent tested age groups, Tukey's test revealed that the value at P21 was significantly lower than those of each individual days from P2 to P12 ( $P < 0.05 - P < 0.001$ ). The value at P17 was also significantly lower than those of P2 and individual days from P4 to P7 ( $P < 0.05$ ).

**2.2.2. GlyR $\alpha$ 2-immunoreactive neurons in the Amb**—GlyR 2-ir was present in ~ 55% - 65% of Amb neurons (Fig. 3G-J). The expression was relatively high from P2 to P5, but declined gradually thereafter until P21 (Fig. 4B). Tukey's test indicated that the levels at P17 and P21 were significantly lower than those at each day tested from P2 to P10 ( $P < 0.05 - P < 0.001$ ). The value at P21 was also lower than those at P11, P12, or P13 ( $P < 0.05$ ). The levels at P13-14 were also lower than that at P5 ( $P < 0.01$  and  $P < 0.001$ , respectively).

**2.2.3. GlyR $\alpha$ 2-immunoreactive neurons in the XII**—About 75% - 85% of the XII neurons exhibited GlyR 2-ir (Fig. 3K-N). The level was relatively high from P2 to P7, but declined gradually thereafter until P21 (Fig. 4C). Tukey's test revealed significant differences between P17 or P21 and each tested day from P2 to P11 ( $P < 0.05 - P < 0.001$ , except for a lack of significance between P11 and P17), and between P7 and P14.

**2.2.4. GlyR $\alpha$ 2-immunoreactive neurons in the NTS<sub>VL</sub>**—GlyR 2-ir was present in ~ 35% - 45% of the NTS<sub>VL</sub> neurons (Fig. 3O-R). The expression followed a trend similar to those of the other three nuclear groups, with relatively high levels from P2 to P10 and a gradual decline until P21 (Fig. 4D). Tukey's test yielded significant differences between P10 and P14, P17, and P21 ( $P < 0.05$ ).

**2.2.5. GlyR $\alpha$ 2-immunoreactive neurons in the CN**—GlyR 2-ir was observed in ~ 30% - 35% of the CN neurons (Fig. 3S-V). The expression was relatively constant with minor fluctuations from P2 to P21, with the lowest levels at P17-21 (Fig. 4E). Tukey's test did not show significant differences between any two age groups.

Two-way ANOVA indicated significant differences in GlyR 2 expression among the five nuclear groups ( $P < 0.01$ ). Subsequent Tukey's tests revealed that the values were significantly higher in Amb than in NTS<sub>VL</sub> at P5 ( $P < 0.05 - P < 0.01$ ), and higher in XII than in NTS<sub>VL</sub> at P7 ( $P < 0.05$  for both).

### 2.3. GlyR $\alpha$ 3-immunoreactive neurons in the brain stem nuclear groups

GlyR 3-ir product was clearly observed in subpopulations of neurons in each of the brain stem nuclear group examined (Fig. 5A, B). Labeling was present in cell bodies and proximal dendrites of neurons as well as in the neuropil. The plasma membrane of many labeled neurons showed clear immunoreaction product (see insets in Fig. 5). Control sections demonstrated no specific immunoreactive product above background (data not shown). One-way ANOVA indicated significant differences in GlyR 3-ir among the ages in the PBC, Amb, XII, and NTS<sub>VL</sub> ( $P < 0.01$ ). However, Tukey's test did not yield significant differences between any two adjacent tested age groups.

**2.3.1. GlyR $\alpha$ 3-immunoreactive neurons in the PBC**—GlyR 3-ir was seen in ~ 50% - 65% of the PBC neurons (Fig. 5C-F). The expression of GlyR 3 was relatively high from P2 to P12, followed by a gradual decline until P21 (Fig. 6A). Tukey's test revealed a significant difference between the much lower value at P21 and those at each of the tested days from P2 to P12 ( $P < 0.01 - P < 0.001$ ), and between the much lower value at P17 and those at P2, P7, and P10 ( $P < 0.05$  for all).

**2.3.2. GlyR $\alpha$ 3-immunoreactive neurons in the Amb**—About 60% - 75% of the Amb neurons were GlyR 3-ir (Fig. 5G-J). The expression was relatively high from P2 to P12 but declined gradually until P21 (Fig. 6B). Tukey's test yielded significant differences between the much lower value at P21 and each of the tested days from P2 to P12 ( $P < 0.05 - P < 0.01$ ), and P17's value was much lower than that at P2 ( $P < 0.05$ ).

**2.3.3. GlyR $\alpha$ 3-immunoreactive neurons in the XII**—GlyR 3-ir was present in ~ 70% - 85% of the XII neurons (Fig. 5K-N). Labeling was relatively high from P2 to P12, but declined gradually until P21 (Fig. 6C). Tukey's test indicated that the expression at P21 was significantly lower than those at each tested days from P2 to P10 ( $P < 0.05 - P < 0.01$ ), and between the much lower values at P13 or P17 and that at P2 ( $P < 0.05$ ).

**2.3.4. GlyR $\alpha$ 3-immunoreactive neurons in the NTS<sub>VL</sub>**—GlyR 3-ir was observed in ~ 40% - 55% of the NTS<sub>VL</sub> neurons (Fig. 5O-R). The expression followed a trend similar to those of the other three nuclear groups, with a relatively high level from P2 to P12, followed by a gradual decline until P21 (Fig. 6D). Tukey's test revealed that the value at P21 was significantly lower than those at each of the tested days at P2, P5, P10, P11, and P12 ( $P < 0.05$ ), and the value at P17 was lower than that at P2 ( $P < 0.05$ ).

**2.3.5. GlyR $\alpha$ 3-immunoreactive neurons in the CN**—GlyR  $\alpha$ 3-ir was present in ~ 50% - 60% of the CN neurons (Fig. 5S-V). The expression was relatively stable between P2 and P21, with the lowest levels at P17-21 (Fig. 6E). Tukey's test did not yield significant differences between any two age groups.

Two-way ANOVA indicated significant differences in GlyR  $\alpha$ 3 expression among the five nuclear groups ( $P < 0.01$ ). Subsequent Tukey's tests revealed that the values were significantly higher in XII than in NTS<sub>VL</sub> at P2, P3, P4, and P7 ( $P < 0.05 - P < 0.01$ ).

## 2.4. GlyR $\beta$ -immunoreactive neurons in the brain stem nuclear groups

GlyR  $\beta$ -ir product was clearly demonstrable in subpopulations of neurons in each of the brain stem nuclear group examined (Fig. 7A, B). Labeling was present in cell bodies and proximal dendrites of neurons as well as in the neuropil. The plasma membrane of many labeled neurons showed immunoreactions product (see insets in Fig. 7). Control sections had no specific labeling above background (data not shown). One-way ANOVA indicated significant differences in GlyR  $\beta$ -ir among the ages in all five nuclear groups examined ( $P < 0.01$ ). However, Tukey's test did not yield significant differences between any two adjacent tested age groups. Significances between non-adjacent age groups are detailed below.

**2.4.1. GlyR $\beta$ -immunoreactive neurons in the PBC**—GlyR  $\beta$ -ir was present in ~ 50% - 70% of the PBC neurons (Fig. 7C-F). The expression was lowest at P2 but rose gradually to reach a peak at P10, followed by a plateau until P21 (Fig. 8A). Tukey's test revealed that the values at each tested day from P7 to P14 was significantly higher than that at P2 ( $P < 0.05 - P < 0.01$ ), and that the value at P10 was significantly higher than that at P3 ( $P < 0.05$ ).

**2.4.2. GlyR $\beta$ -immunoreactive neurons in the Amb**—GlyR  $\beta$ -ir was observed in ~ 55% - 75% of the Amb neurons (Fig. 7G-J). The expression was the lowest at P2, but rose gradually to peak at P11-12, followed by a gradual decline until P21 (Fig. 8B). Tukey's test showed that the expression at P11 and P12 was significantly higher than that at P2 ( $P < 0.05$ ).

**2.4.3. GlyR $\beta$ -immunoreactive neurons in the XII**—About 75% - 85% of the XII neurons exhibited GlyR  $\beta$ -ir (Fig. 7K-N). The expression was again the lowest at P2, rose gradually to peak at P12, followed by a gradual decline until P21 (Fig. 8C). Tukey's test indicated that the expression at P12 was significantly higher than those at each tested days at P2, P3, P4, P17, and P21 ( $P < 0.05 - P < 0.001$ ), and the value at P11 was much higher than those at P2 and P3 ( $P < 0.01$  or  $P < 0.05$ , respectively).

**2.4.4. GlyR $\beta$ -immunoreactive neurons in the NTS<sub>VL</sub>**—GlyR  $\beta$ -ir was present in ~ 40% - 50% of the XII neurons (Fig. 7O-R). The trend of expression was similar to those of the other three nuclear groups, in that the level was lowest at P2, then rose gradually to reach a peak at P12, followed by a gradual decline until P21 (Fig. 8D). Tukey's test showed that the expression at P12 was significantly higher than those at P2, P3, P4, P17, or P21 ( $P < 0.05 - P < 0.001$ ), and that the value at P13 was significantly higher than those at P2 and P4 ( $P < 0.05$ ).

**2.4.5. GlyR $\beta$ -immunoreactive neurons in the CN**—Approximately 35% - 45% of the CN neurons demonstrated GlyR  $\beta$ -ir (Fig. 7S-V). The expression followed a trend similar to those in the Amb, XII, and NTS<sub>VL</sub>, with the lowest level at P2, a gradual rise to peak at P12, followed by a gradual decline until P21 (Fig. 8E). Tukey's test revealed that the expression at each tested day from P11 to P14 was significantly higher than those at P2, P3, P4, or P21

( $P < 0.05$  –  $P < 0.001$ , except for a lack of significance between P14 and P21), and the value at P12 was significantly higher than those at P5 or P17 ( $P < 0.05$ ).

Two-way ANOVA indicated significant differences in GlyR expression among the five nuclear groups ( $P < 0.01$ ). Subsequent Tukey's tests revealed that the values were significantly higher in XII than in NTS<sub>VL</sub> at P4-12, P17, and P21 ( $P < 0.05$  –  $P < 0.01$ ).

### 3. Discussion

The present large-scale, in-depth developmental study revealed for the first time that: 1) the expression of GlyR  $\alpha 1$  increased with age in four respiratory-related nuclear groups, and reached the only day-to-day significant increase at P12, the height of the critical period; 2) the expressions of GlyR  $\alpha 2$  and GlyR  $\alpha 3$  in the four nuclear groups were relatively high at P2 but declined after the first 1 to 1 ½ weeks to reach the lowest level at P21; 3) the expression of GlyR  $\alpha 4$  followed closely that of GlyR  $\alpha 1$  in that the level increased with age; however, there was not a day-to-day significant increase at P12; and 4) in the non-respiratory cuneate nucleus, the expressions of GlyR  $\alpha 1$ - $\alpha 3$  had a much gentler rise and fall with age, whereas that of GlyR  $\alpha 4$  was comparable to those in the other four nuclear groups. Thus, our results strongly support our hypothesis that a developmental switch in GlyR subunits (from GlyR  $\alpha 2$  and/or GlyR  $\alpha 3$  to GlyR  $\alpha 1$ ) occurs in respiratory-related nuclear groups around the critical period (P12). The developmental increase in the expression of GlyR  $\alpha 4$  suggests that it contributes to a heteromeric  $\alpha 4$  subunit composition in mature glycine receptors.

#### 3.1. Functions of glycine receptors

Glycine is one of the two major inhibitory neurotransmitters in the central nervous system (Aprison and Daly, 1978). Like GABA, glycine is critical for fast synaptic inhibition in the brain stem respiratory system and is essential for normal respiratory pattern generation by controlling respiratory phase transitions during pre- and postinspiration in the neonate and in the adult (Schmid et al., 1991; Paton and Richter, 1995; Shao and Feldman, 1997; Büsselberg et al., 2001; Dutschmann and Paton, 2002). Although glycinergic pacemaker neurons have been found in the PBC (Morgado-Valle et al., 2010), they are few in number, and inhibition is considered not necessary for inspiratory rhythmogenesis in the PBC (Feldman et al., 2013). Glycinergic inhibition is essential for coordinating the activity of breathing and upper airway patency that involves Amb and XII motoneurons (Singer et al., 1998; Dutschmann and Paton, 2002). Inhibitory pump cells in the NTS<sub>VL</sub> of rats adjust respiratory control in response to lung volume changes, including the Breuer-Hering reflex (Ezure and Tanaka, 2004; Kubin et al., 2006; Janczewski et al., 2013). Rat pump cells also receive a phasic inhibitory input at the transition from inspiration to expiration, and glycinergic inhibition is involved during early inspiration (Miyazaki et al., 1999). With hypoxia, glycine is thought to be involved in the late, depressive phase of the hypoxic ventilatory response (Kato et al., 2000).

In many regions of the brain, both glycine and GABA transition postnatally from an initial depolarizing, excitatory phase to a mature hyperpolarizing inhibitory one (Fulton et al., 1980; Ben-Ari et al., 1989; Owens et al., 1996; Bakus et al., 1998). In the rat respiratory system, such transition occurs during the first two postnatal weeks in hypoglossal motoneurons, coincidental with a switch in GlyR subunit mRNAs from  $\alpha 2$  to  $\alpha 1$  (Singer et al., 1998). However, in the PBC, the transition reportedly occurs at embryonic day 19 (Ren and Greer, 2006). A postnatal switch from the neonatal GABA<sub>A</sub> receptor  $\alpha 3$  to the mature  $\alpha 1$  (Liu and Wong-Riley, 2004, 2006) and from GlyR  $\alpha 2/\alpha 3$  to GlyR  $\alpha 1$  (present study) are consistent with postnatal maturation of Cl<sup>-</sup>-mediated synaptic transmission in multiple respiratory-related nuclear groups in the brain stem. However, they do not directly address the question of depolarization versus hyperpolarization events.

The action of glycine is mediated through its pentameric ligand-gated Cl<sup>-</sup> channel receptors (Betz and Becker, 1988). These receptors belong to the Cys loop receptor family, which includes nicotinic acetylcholine receptors (nAChR), GABA<sub>A</sub> receptors (GABA<sub>A</sub>R), and serotonergic type 3 receptors (5-HT<sub>3</sub>R) (Dutertre et al., 2012). Five genes have been identified for GlyRs:  $\alpha 1$ - $\alpha 4$  and a single  $\beta$  gene (reviewed in Kuhse et al., 1991). All subunits share high sequence identity (> 80%), are ~ 48 kDa in molecular weight, provide the ligand-binding motif, and can form homomeric receptors. The  $\alpha$  subunit, on the other hand, is ~58 kDa, can only form heteromers with  $\beta$  subunits, contributes to agonist binding, and interacts with gephyrin to enhance GlyR clustering at the synapse (Meyer et al., 1995; Kneussel and Betz, 2000; Maas et al., 2006).

### 3.2. Developmental changes in glycine receptor subunit expression

**3.2.1. GlyR $\alpha 2$** —The higher expression of GlyR  $\alpha 2$  during the first postnatal week and its decline with age in all four respiratory-related nuclear groups is consistent with this subunit being regarded as the embryonic or neonatal form, whose level declines rapidly by the 3<sup>rd</sup> postnatal week (Becker et al., 1988; Malosio et al., 1991; Watanabe and Akagi, 1995; Lynch, 2009). GlyR  $\alpha 2$ s mediate inhibitory postsynaptic currents (IPSCs) that have slow decay kinetics (Dutertre et al., 2012). This is reminiscent of the longer decay time of the glycine-mediated miniature IPSCs during the first postnatal week in hypoglossal motoneurons (Gao et al., 2011). GlyR  $\alpha 2$ s form homomeric receptors that are localized to extrasynaptic sites and rely on paracrine glycine and taurine signaling to provide a slow, tonic effect on neurons (Aroeira et al., 2011; Jonsson et al., 2012). As the level of intracellular Cl<sup>-</sup> is kept high by the greater expression of the Cl<sup>-</sup>-intruder Na<sup>+</sup>-K<sup>+</sup>-2Cl<sup>-</sup> co-transporter 1 (NKCC1) in many brain stem respiratory-related neurons (Liu and Wong-Riley, 2012), the homomeric GlyR  $\alpha 2$ s may mediate depolarization that stimulates calcium influx essential for the development of many neuronal properties, including glycinergic synapses (Lynch, 2009). Interestingly enough, GlyR  $\alpha 2$  knock-out mice are phenotypically normal (Young-Pearse et al., 2006).

**3.2.2. GlyR $\alpha 3$** —Although GlyR  $\alpha 3$ , like GlyR  $\alpha 2$ , exhibited an age-dependent decrease in its expression in the four respiratory-related nuclear groups, its reduction did not commence until after P12, i.e., about 2-5 days later than that of GlyR  $\alpha 2$ . This discrepancy in timing implies that  $\alpha 2$  and  $\alpha 3$  are not regulated in synchrony and that  $\alpha 3$  continues to play an important role into the second postnatal week and perhaps later. GlyR  $\alpha 3$  confers medium-fast kinetics that is intermediate between the neonatal slow  $\alpha 2$  and the mature fast  $\alpha 1$  (Weiss et al., 2008). In the respiratory network, the rhythmic activity is affected by the phosphorylation state of GlyR  $\alpha 3$ , which is controlled by serotonergic receptors, specifically 5-HT<sub>1A</sub>R (Manzke et al., 2010; Shevtsova et al., 2011). The 5-HT<sub>1A</sub>R- GlyR  $\alpha 3$  signaling can rescue opioid-induced respiratory depression by glycinergic inhibition of inhibitory neurons, thereby inducing disinhibition (Manzke et al., 2010; Shevtsova et al., 2011). Between P2 and P11, such modulation may be more efficient, as the expressions of both 5-HT 1A and GlyR  $\alpha 3$  are at their highest in several respiratory-related nuclear groups (Liu and Wong-Riley, 2010a, and the present study).

**3.2.3. GlyR $\alpha 1$** —The expression of GlyR  $\alpha 1$  increased with age in all four respiratory-related nuclear groups examined. Thus, this is the predominant isoform that contributes to the mature GlyRs (Lynch, 2009). Remarkably, the expression of GlyR  $\alpha 1$  peaked significantly at P12, at the height of the critical period, in all four respiratory-related nuclear groups. GlyR  $\alpha 1$ -containing receptors mediate inhibitory postsynaptic currents that have short mean open times and fast decay kinetics (Singer et al., 1998). The peaking of GlyR  $\alpha 1$  at P12 implies that at the height of the critical period, glycinergic inhibition is strong within the respiratory network. Consistent with this idea are our findings in hypoglossal

motoneurons that the amplitude, mean frequency and charge transfer of miniature IPSCs are significantly increased at P12-13, that the amplitude and frequency of spontaneous IPSCs are significantly increased at P12-13, and that glycinergic transmission dominates over GABAergic ones after the first postnatal week (Gao et al., 2011).

A point mutation in the *Gla1* gene leads to spasticity (Saul et al., 1994), and *Gla1* null mutation causes fine motor tremor and muscle spasms that begin at the second postnatal week and worsens until death by three weeks of age in mice (Buckwalter et al., 1994). These findings imply that none of the other GlyR subunits can compensate for the loss of GlyR 1 function.

**3.2.4. GlyR $\beta$** —The expression of the  $\beta$  subunit in all five brain stem nuclear groups examined exhibited an age-dependent increase from P2 to P12, peaking at the height of the critical period before down-regulating slightly until P21. This trend is similar though not identical to that of GlyR 1. As  $\beta$  subunits cannot form homomers by themselves, they need  $\alpha$  subunits to generate heteropentamers. Recent experiments indicate that the mature pentamer is made up of 2  $\alpha$  and 3  $\beta$  subunits rather than the 3  $\alpha$  2  $\beta$  model proposed previously (Langosch et al., 1988; Deutertre et al., 2012). As the level of GlyR 3 remained quite high until P12 and that of GlyR 1 did not peak until P12 in the four respiratory-related nuclear groups, it is possible that  $\beta$  subunits form GlyRs with 3 in the few days before the critical period, then with 1 and possibly 3 during the critical period before transitioning to mainly 1. The  $\beta$  subunit determines the ligand-binding property of GlyRs and is essential in anchoring GlyR at synaptic sites (Grudzinska et al., 2005).

### 3.3. Critical period of respiratory development

Glycine is likely to play an important role during the critical period, when heightened inhibition and suppressed excitation demonstrable both neurochemically and electrophysiologically render the respiratory system less capable of responding adequately to hypoxia (Liu and Wong-Riley, 2002, 2005, Liu et al., 2006, 2009; Gao et al., 2011). In addition to a switch in dominance from the neonatal GlyR 2 and/or 3 to the mature GlyR 1 (the present study) that signals a more robust inhibition, the transient rise in inhibition during the critical period is further contributed by several factors occurring concurrently: a) a switch in the dominance of expression from NKCC1 to KCC2, enabling either a transition from depolarizing to hyperpolarizing, or a strengthening of the hyperpolarizing potentials mediated by GABA and glycine receptors (Liu and Wong-Riley, 2012); b) a switch in dominance from the neonatal 3 to the mature 1 for the GABA<sub>A</sub> receptors (Liu and Wong-Riley, 2004, 2006); c) a suppressed expression of multiple serotonergic receptors, serotonin transporter, and serotonin synthesizing enzyme in multiple brain stem respiratory-related nuclear groups (Liu and Wong-Riley, 2008; 2010a,b), which would attenuate the “net stimulatory effect” of serotonin on respiratory output (Lindsay and Feldman, 1993; Hodges and Richerson, 2008); reduced 5-HT<sub>1A</sub>R expression would also imply that its disinhibitory effect on respiration via GlyR 3 (Manzke et al., 2010; Shevtsova et al., 2011) would be diminished; and d) a significant reduction in the expression of brain-derived neurotrophic factor (BDNF) and its high-affinity receptor (tyrosine protein kinase B, TrkB) in multiple respiratory-related nuclear groups (Liu and Wong-Riley, 2013) indicates that their normal enhancement of excitation and suppression of inhibition (Wardle and Poo, 2003) would be reduced. These cumulative effects culminate in a transient state of augmented inhibition during the critical period that eventually subsides into a more balanced state of excitation and inhibition. During this time, the animals’ ventilatory and metabolic responses to acute hypoxia are at their weakest (Liu et al., 2006, 2009). It is also noteworthy that rats challenged with a primary immune system-altering infection and a secondary sublethal dose of endotoxin die mainly on day 12 (Blood-Siegfried et al., 2002). These

findings have special implication for Sudden Infant Death Syndrome (SIDS), as a critical period constitutes one of its three risk factors (Filiano and Kinney, 1994).

## 4. Experimental procedures

### 4.1. Tissue preparation

All experiments and animal procedures were performed in accordance with the Guide for the Care and Use of Laboratory Animals (National Institutes of Health Publications No. 80-23, revised 1996), and all protocols were approved by the Medical College of Wisconsin Animal Care and Use Committee (approval can be provided upon request). All efforts were made to minimize the number of animals used and their suffering.

A total of 96 Sprague-Dawley rats, both male and female, from 8 litters were used. Rat pups were sacrificed at each of postnatal days P2, 3, 4, 5, 7, 10, 11, 12, 13, 14, 17, and 21. They were deeply anesthetized with 0.6% sodium pentobarbital (60 mg/kg IP; Diamondback drugs, Scottsdale, AZ) and perfused through the aorta with 4% paraformaldehyde-4% sucrose in 0.1 M sodium phosphate buffered saline (PBS), pH 7.4. Brain stems were then removed, postfixed in the same fixative for 3 h at 4°C, cryoprotected by immersion in increasing concentrations of sucrose (10, 20, and 30%) in 0.1 M PBS at 4°C, then frozen on dry ice and stored at -80°C until use.

### 4.2. Characterization of antibodies

Table 1 shows a summary of the antibodies used in the present study. The anti-GlyR<sub>1</sub> was an affinity purified rabbit polyclonal antibody raised against the human synthetic GlyR<sub>1</sub> peptide of 24 amino acids (between aa 190 and 239), and it yielded a single band of ~ 48 kDa by western blot analysis (manufacturer's datasheet). The anti-GlyR<sub>2</sub> was a rabbit polyclonal antibody raised against the human C-terminus of GlyR<sub>2</sub> (between aa 371 and 420), and it yielded a single band at ~ 48 kDa by western blot analysis (manufacturer's datasheet). Previous immunohistochemical study showed specific labeling of GlyR<sub>2</sub> (García-Alcocer et al., 2008). The anti-GlyR<sub>3</sub> was an affinity-purified goat polyclonal antibody raised against a 15 amino acid synthetic peptide between aa 400-450 of the C-terminus of human GlyR<sub>3</sub>, and it yielded a single band at ~ 48 kDa by western blot analysis (manufacturer's datasheet). In transfected HEK293T cells, the GlyR<sub>3</sub> antibody recognizes only the recombinant rat GlyR<sub>3</sub> protein and not GlyR<sub>1</sub>, <sub>2</sub>, or <sub>4</sub> subunits (Weltzien et al., 2012). Immunohistochemical studies showed specific labeling of GlyR<sub>3</sub> with this antibody (Majumdar et al., 2007; García-Alcocer et al., 2008; Weiss et al., 2008), and the staining was abolished in tissues of GlyR<sub>3</sub> knockout mice (Heinze et al., 2007). The anti-GlyR<sub>4</sub> was an affinity-purified goat polyclonal antibody raised against a 20 amino acid synthetic peptide between aa 400-450 of the C-terminus of human GlyR<sub>4</sub>, and it yielded a single band at ~ 58 kDa by western blot analysis (manufacturer's datasheet and Laterza et al., 2006). Its specificity was also shown in immunohistochemical studies (García-Alcocer et al., 2008). The genes encoding human GlyR<sub>1</sub>, <sub>2</sub>, <sub>3</sub>, and <sub>4</sub> have been mapped to chromosomes 5q31.3, Xp21.2-22.1, 4q32, and 4q33-34, respectively (Grenningloh et al., 1990; Handford et al., 1996; Nikolic et al., 1998).

### 4.3. Immunohistochemistry

Coronal sections (12-µm thickness) of frozen brain stems were cut with a Leica CM1900 cryostat (Leica Microsystems, Heidelberg, Nussloch, Germany). Individual sets of serial sections were mounted on gelatin-coated slides. In the same litter, sections from 3 rats at different ages were mounted on the same slides and processed together. Ages were grouped typically as follows: P2-10-21, P3-4-17, P5-7-14, and P11-12-13. All sections from all rats were processed under identical conditions (i.e., time, temperature, and concentration of

reagents). They were blocked overnight at 4°C with 5% nonfat dry milk-5% normal goat serum-1% Triton X-100 in 0.1 M PBS (pH 7.4). Alternating sets of sections were then incubated at 4°C for 36 h in one of the primary antibodies diluted at the proper concentration in the same solution as used for blocking (see Table 1 for antibodies' concentration). Sections were rinsed 3 times, 5 min each, in PBS, then incubated in the secondary antibodies: 1:100 goat anti-rabbit IgG-HRP (Bio-Rad, Hercules, CA) for GlyR 1, GlyR 2, and 1:100 rabbit anti-goat IgG-HRP (Millipore Corp, Temecula, CA) for GlyR 3 and GlyR , diluted in the modified blocking solution (without Triton X-100) for 4 h at room temperature. After rinsing twice with PBS and once with 0.1 M ammonium phosphate buffer (APB), pH 7.0, immunoreactivity was detected with 0.05% DAB-0.004% H<sub>2</sub>O<sub>2</sub> in APB for 5 min. The reaction was then stopped with APB for 5 min, rinsed in PBS three times, dehydrated, and coverslipped. Control sections were processed without primary antibodies or with a non-immune serum in place of the primary antibodies.

#### 4.4. Semi-quantitative optical densitometry

The immunoreactivity of GlyR 1, 2, 3, and in the cell bodies of individual neurons in various nuclear groups was semi-quantitatively analyzed by optical densitometry performed with a Zeiss Zonax MPM 03 photometer, a ×25 objective, and a 2-μm-diameter measuring spot. White (tungsten) light was used for illumination, and all lighting conditions were held constant for all of the measurements. Since light intensity can directly affect optical densitometric values, a stepped density filter (Edmund Industrial Optics, Barrington, NJ) with 10-step increments of 0.1 (from 0.1 to 1) was used to precisely adjust the intensity of the light source to a standard value identical for all samples.

The boundary of each brain stem nuclear group studied was determined with the aid of the Paxinos and Watson's "The Rat Brain Atlas" (Academic Press, New York, 1986). The PBC was identified with the neurokinin-1 receptor labeling (Gray et al., 1999), its rostral and caudal boundary was determined according to the detailed descriptions of Smith et al. (1991), and as described in our previous papers (Liu and Wong-Riley, 2002, 2005). The part of the nucleus ambiguus chosen for the present study was the semicompact formation and the rostral loose formation innervating upper airway muscles with pharyngolaryngomotor functions (Bieger and Hopkins, 1987). For the remaining nuclear groups, measurements were taken from the central main portion of each nuclear group. The optical densitometric value of each neuron measured was an average of two to four spots (depending on the cell size) within the cytoplasm (avoiding the nucleus). About 100 neurons in each brain stem nuclear group were measured for each marker in each rat, and a total of about 800 neurons at each age for each marker were measured. For statistical analyses, each sample's optical density value for each nuclear group of each rat was the average of about 100 labeled neurons. A total of 192,000 neurons were measured for the present study. Mean optical density values, standard deviations, and standard errors of the mean in each nuclear group at each age were then obtained. Statistical comparisons were made among the age groups by using one-way analysis of variance (ANOVA) (to control for the type I comparisonwise error rate) and, when significant differences were found, comparisons were made between successive age groups (e.g., P2 vs. P3, P3 vs. P4, and P5 vs. P7) by using Tukey's Studentized range test (a *post hoc* multiple comparisons, to control for the type I experimentwise error rate). Additional Tukey's tests were conducted between two groups that were not immediately adjacent to each other, and significant differences, if any, were presented in the Results section (but not shown in the graphs to minimize confusion). Two-way ANOVA was also done to determine if there was differential expression across nuclear groups, and when significance was found, Tukey's test was then done to determine when and where such differences were found. Significance was set at  $P < 0.01$  for one- or two-way ANOVA and  $P < 0.05$  for Tukey's test.

The percentage of labeled neurons for each glycinergic subunit in each nuclear group was calculated based on the number of labeled neurons divided by the total number of neurons shown in adjacent Nissl stained sections through the entire extent of each nuclear group. Only neurons sectioned through their centers (i.e., with clear nucleus) were counted. The range of percentages during development was based on values obtained at P2, P7, P12, and P21.

## Acknowledgments

This study was supported by a grant from National Institutes of Health, grant number: R01 HD048954.

Role of authors

Both authors have full access to all the data in the study and take responsibility for the integrity of the data and the accuracy of the data analysis.

## Abbreviations

<b>5-HT</b>	serotonin
<b>XII</b>	hypoglossal nucleus
<b>Amb</b>	nucleus ambiguus
<b>ANOVA</b>	analysis of variance
<b>APB</b>	ammonium phosphate buffer
<b>BDNF</b>	brain-derived neurotrophic factor
<b>CN</b>	cuneate nucleus
<b>CNS</b>	central nervous system
<b>GABA</b>	gamma aminobutyric acid
<b>GlyR</b>	glycine receptor
<b>IgG-HRP</b>	immunoglobulin conjugated to horseradish peroxidase
<b>IPSC</b>	inhibitory postsynaptic currents
<b>ir</b>	immunoreactive
<b>KCC2</b>	K <sup>+</sup> -Cl <sup>-</sup> co-transporter 2
<b>NK1R</b>	neurokinin 1 receptor
<b>NKCC1</b>	Na <sup>+</sup> -K <sup>+</sup> -2Cl <sup>-</sup> co-transporter 1
<b>NMDAR</b>	N-methyl-D-aspartate receptor
<b>NTS<sub>VL</sub></b>	ventrolateral subnucleus of the solitary tract nucleus
<b>P</b>	postnatal day
<b>PBC</b>	pre-Bötzinger complex
<b>PBS</b>	phosphate buffered saline
<b>TrkB</b>	tyrosine protein kinase B

## LITERATURE CITED

Aprison MH, Daly EC. Biochemical aspects of transmission at inhibitory synapses: the role of glycine. *Adv. Neurochem.* 1978; 3:203–294.

- Aroeira RI, Ribeiro JA, Sebastião AM, Valente CA. Age-related changes of glycine receptor at the rat hippocampus: from the embryo to the adult. *J. Neurochem.* 2011; 118:339–353. [PubMed: 21272003]
- Bakus KH, Deitmer JW, Friauf E. Glycine-activated currents are changed by coincident membrane depolarization in developing rat auditory brainstem neurons. *J. Physiol. (Lond).* 1998; 507:783–794. [PubMed: 9508839]
- Becker CM, Hoch W, Betz H. Glycine receptor heterogeneity in rat spinal cord during postnatal development. *EMBO J.* 1988; 7:3717–3726. [PubMed: 2850172]
- Ben-Ari Y, Cherubini E, Corradetti R, Gaiarsa JL. Giant synapse potentials in immature rat CA3 hippocampal neurons. *J. Physiol. (Lond).* 1989; 416:303–325. [PubMed: 2575165]
- Betz H, Becker CM. The mammalian glycine receptor: biology and structure of a neuronal chloride channel protein. *Neurochem. Int.* 1988; 13:137–146. [PubMed: 20501281]
- Bieger D, Hopkins DA. Viscerotopic representation of the upper alimentary tract in the medulla oblongata in the rat: the nucleus ambiguus. *J. Comp. Neurol.* 1987; 262:546–562. [PubMed: 3667964]
- Blood-Siegfried J, Nyska A, Lieder H, Joe M, Vega L, Patterson R, Germolec D. Synergistic effect of influenza A virus on endotoxin-induced mortality in rat pups: a potential model for sudden infant death syndrome. *Pediatr. Res.* 2002; 52:481–490. [PubMed: 12357040]
- Bonham AC. Neurotransmitters in the CNS control of breathing. *Respir. Physiol.* 1995; 101:219–230. [PubMed: 8606995]
- Buckwalter MS, Cook SA, Davisson MT, White WF, Camper SA. A frameshift mutation in the mouse alpha 1 glycine receptor gene (*Glr1*) results in progressive neurological symptoms and juvenile death. *Hum. Mol. Genet.* 1994; 3:2025–2030. [PubMed: 7874121]
- Büsselberg D, Bischoff AM, Paton JF, Richter DW. Reorganisation of respiratory network activity after loss of glycinergic inhibition. *Pflugers Arch.* 2001; 441:444–449. [PubMed: 11212206]
- Dutertre S, Becker CM, Betz H. Inhibitory glycine receptors: an update. *J. Biol. Chem.* 2012; 287:40216–40223. [PubMed: 23038260]
- Dutschmann M, Paton JF. Glycinergic inhibition is essential for co-ordinating cranial and spinal respiratory motor outputs in the neonatal rat. *J. Physiol.* 2002; 543:643–653. [PubMed: 12205196]
- Ellenberger HH, Feldman JL. Brainstem connections of the rostral ventral respiratory group of the rat. *Brain. Res.* 1990; 513:35–42. [PubMed: 2350683]
- Ezure K, Tanaka I. GABA, in some cases together with glycine, is used as the inhibitory transmitter by pump cells in the Hering-Breuer reflex pathway of the rat. *Neurosci.* 2004; 127:409–417.
- Feldman JL, Del Negro CA, Gray PA. Understanding the rhythm of breathing: so near, yet so far. *Annu. Rev. Physiol.* 2013; 75:423–452. [PubMed: 23121137]
- Filiano JJ, Kinney HC. A perspective on neuropathologic findings in victims of the sudden infant death syndrome: the triple-risk model. *Biol. Neonate.* 1994; 65:194–197. [PubMed: 8038282]
- Finley JCW, Katz DM. The central organization of carotid body afferent projection to the brain stem of the rat. *Brain. Res.* 1992; 572:108–116. [PubMed: 1611506]
- Fulton BP, Miledi R, Takahashi T. Electrical synapses between motoneurons in the spinal cord of the newborn rat. *Proc. R. Soc. Lond. B. Biol. Sci.* 1980; 208:115–120. [PubMed: 6105652]
- Gao XP, Liu QS, Liu Q, Wong-Riley MTT. Excitatory-inhibitory imbalance in hypoglossal neurons during the critical period of postnatal development in the rat. *J. Physiol.* 2011; 589:1991–2006. [PubMed: 21486774]
- García-Alcocer G, Mejía C, Berumen LC, Miledi R, Martínez-Torres A. Developmental expression of glycine receptor subunits in rat cerebellum. *Int. J. Dev. Neurosci.* 2008; 26:319–322. [PubMed: 18339511]
- Gray PA, Rekling JC, Bocchiaro CM, Feldman JL. Modulation of respiratory frequency by peptidergic input to rhythmogenic neurons in the pre-Bötzinger complex. *Science.* 1999; 286:1566–1568. [PubMed: 10567264]
- Greeningloh G, Schmieden V, Schofield PR, Seeburg PH, Siddique T, Mohandas TK, Becker CM, Betz H. Alpha subunit variants of the human glycine receptor: primary structures, functional expression and chromosomal localization of the corresponding genes. *EMBO J.* 1990; 9:771–776. [PubMed: 2155780]

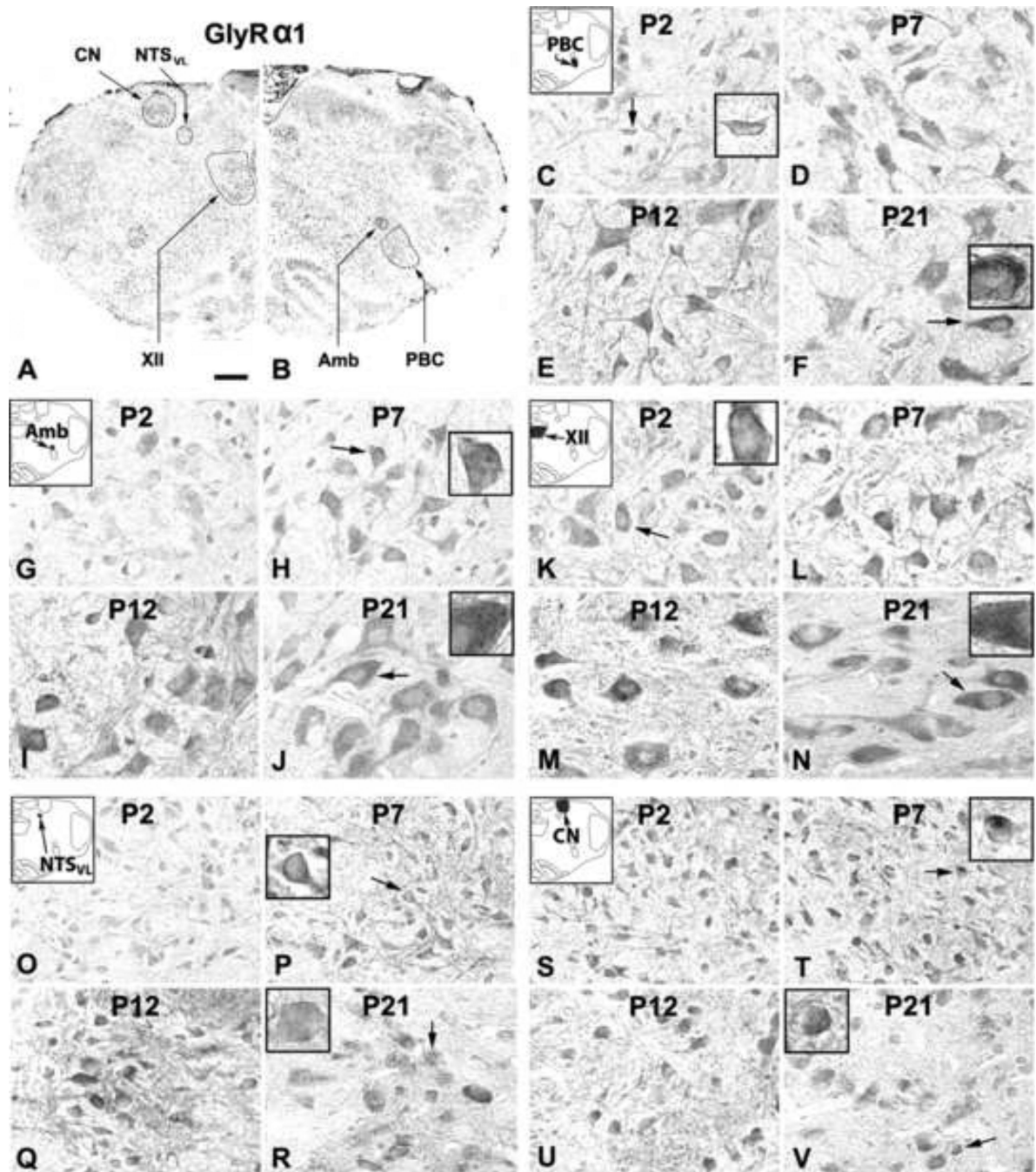
- Grudzinska J, Schemm R, Haeger S, Nicke A, Schmalzing G, Betz H, Laube B. The beta subunit determines the ligand binding properties of synaptic glycine receptors. *Neuron*. 2005; 45:727–739. [PubMed: 15748848]
- Handford CA, Lynch JW, Baker E, Webb GC, Ford JH, Sutherland GR, Schofield PR. The human glycine receptor beta subunit: primary structure, functional characterisation and chromosomal localisation of the human and murine genes. *Brain Res. Mol. Brain Res.* 1996; 35:211–219. [PubMed: 8717357]
- Heinze L, Harvey RJ, Haverkamp S, Wässle H. Diversity of glycine receptors in the mouse retina: localization of the alpha4 subunit. *J. Comp. Neurol.* 2007; 500:693–707. [PubMed: 17154252]
- Hodges MR, Richerson GB. Contributions of 5-HT neurons to respiratory control: neuromodulatory and trophic effects. *Respir. Physiol. Neurobiol.* 2008; 164:222–232. [PubMed: 18595785]
- Holtman JR Jr, Marion LJ, Speck DF. Origin of serotonin-containing projections to the ventral respiratory group in the rat. *Neurosci.* 1990; 37:541–552.
- Janczewski WA, Tashima A, Hsu P, Cui Y, Feldman JL. Role of inhibition in respiratory pattern generation. *J. Neurosci.* 2013; 33:5454–5465. [PubMed: 23536061]
- Jonsson S, Morud J, Pickering C, Adermark L, Ericson M, Söderpalm B. Changes in glycine receptor subunit expression in forebrain regions of the Wistar rat over development. *Brain Res.* 2012; 1446:12–21. [PubMed: 22330726]
- Jordan D. Central nervous pathways and control of the airways. *Respir. Physiol.* 2001; 125:67–81. [PubMed: 11240153]
- Kato T, Hayashi F, Tatsumi K, Kuriyama T, Fukuda Y. Inhibitory mechanisms in hypoxic respiratory depression studied in an in vitro preparation. *Neurosci. Res.* 2000; 38:281–288. [PubMed: 11070195]
- Kneussel M, Betz H. Clustering of inhibitory neurotransmitter receptors at developing postsynaptic sites: the membrane activation model. *Trends Neurosci.* 2000; 23:429–435. [PubMed: 10941193]
- Kubin L, Alheid GF, Zuperku EJ, McCrimmon DR. Central pathways of pulmonary and lower airway vagal afferents. *J. Appl. Physiol.* 2006; 101:618–627. [PubMed: 16645192]
- Kuhse J, Becker CM, Schmieden V, Hoch W, Pribilia I, Langosch D, Malosio ML, Muntz M, Betz H. Heterogeneity of the inhibitory glycine receptor. *Ann. N Y Acad. Sci.* 1991; 625:129–135. [PubMed: 1647720]
- Langosch D, Thomas L, Betz H. Conserved quaternary structure of ligand-gated ion channels: the postsynaptic glycine receptor is a pentamer. *Proc. Natl. Acad. Sci. USA.* 1988; 85:7394–7398. [PubMed: 2459705]
- Laterza OF, Modur VR, Crimmins DL, Olander JV, Landt Y, Lee JM, Ladenson JH. Identification of novel brain biomarkers. *Clin. Chem.* 2006; 52:1713–1721. [PubMed: 16858073]
- Lindsay AD, Feldman JL. Modulation of respiratory activity of neonatal rat phrenic motoneurons by serotonin. *J. Physiol.* 1993; 461:213–233. [PubMed: 8350262]
- Liu Q, Wong-Riley MTT. Postnatal expression of neurotransmitters, receptors, and cytochrome oxidase in the rat pre-Bötzinger complex. *J. Appl. Physiol.* 2002; 92:923–934. [PubMed: 11842022]
- Liu Q, Wong-Riley MTT. Developmental changes in the expression of GABAA receptor subunits alpha1, alpha2, and alpha3 in the rat pre-Bötzinger complex. *J. Appl. Physiol.* 2004; 96:1825–1831. [PubMed: 14729731]
- Liu Q, Wong-Riley MTT. Postnatal developmental expressions of neurotransmitters and receptors in various brain stem nuclei of rats. *J. Appl. Physiol.* 2005; 98:1442–1457. [PubMed: 15618314]
- Liu Q, Wong-Riley MTT. Developmental changes in the expression of GABAA receptor subunits alpha1, alpha2, and alpha3 in brain stem nuclei of rats. *Brain Res.* 2006; 1098:129–138. [PubMed: 16750519]
- Liu Q, Wong-Riley MTT. Postnatal changes in the expression of serotonin 2A receptors in various brain stem nuclei of the rat. *J. Appl. Physiol.* 2008; 104:1801–1808. [PubMed: 18420721]
- Liu Q, Wong-Riley MTT. Postnatal changes in the expressions of serotonin 1A, 1B, and 2A receptors in ten brain stem nuclei of the rat: implication for a sensitive period. *Neurosci.* 2010a; 165:61–78.

- Liu Q, Wong-Riley MTT. Postnatal changes in tryptophan hydroxylase and serotonin transporter immunoreactivity in multiple brainstem nuclei of the rat: implications for a sensitive period. *J. Comp. Neurol.* 2010b; 518:1082–1097. [PubMed: 20127812]
- Liu Q, Wong-Riley MTT. Postnatal development of Na<sup>+</sup>-K<sup>+</sup>-2Cl<sup>-</sup> co-transporter 1 and K<sup>+</sup>-Cl<sup>-</sup> co-transporter 2 immunoreactivity in multiple brain stem respiratory nuclei of the rat. *Neurosci.* 2012; 210:1–20.
- Liu Q, Wong-Riley MTT. Postnatal development of brain-derived neurotrophic factor (BDNF) and tyrosine protein kinase B (TrkB) receptor immunoreactivity in multiple brain stem respiratory-related nuclei of the rat. *J. Comp. Neurol.* 2013; 521:109–129. [PubMed: 22678720]
- Liu Q, Lowry TF, Wong-Riley MTT. Postnatal changes in ventilation during normoxia and acute hypoxia in the rat: implication for a sensitive period. *J. Physiol.* 2006; 577:957–970. [PubMed: 17038423]
- Liu Q, Fehring C, Lowry TF, Wong-Riley MTT. Postnatal development of metabolic rate during normoxia and acute hypoxia in rats: implication for a sensitive period. *J. Appl. Physiol.* 2009; 106:1212–1222.
- Lowe AA. The neural regulation of tongue movements. *Prog. Neurobiol.* 1980; 15:295–344. [PubMed: 7244250]
- Lynch JW. Native glycine receptor subtypes and their physiological roles. *Neuropharmacol.* 2009; 56:303–309.
- Maas C, Tagnaouti N, Loeblich S, Behrend B, Lappe-Siefke C, Kneussel M. Neuronal cotransport of glycine receptor and the scaffold protein gephyrin. *J. Cell Biol.* 2006; 172:441–451. [PubMed: 16449194]
- Majumdar S, Heinze L, Haverkamp S, Ivanova E, Wässle H. Glycine receptors of A-type ganglion cells of the mouse retina. *Vis. Neurosci.* 2007; 24:471–487. [PubMed: 17550639]
- Malosio ML, Marquèze-Pouey B, Kuhse J, Betz H. Widespread expression of glycine receptor subunit mRNAs in the adult and developing rat brain. *EMBO J.* 1991; 10:2401–2409. [PubMed: 1651228]
- Manzke T, Niebert M, Koch UR, Caley A, Vogelgesang S, Hülsmann S, Ponimaskin E, Müller U, Smart TG, Harvey RJ, Richter DW. Serotonin receptor 1A-modulated phosphorylation of glycine receptor  $\alpha$ 3 controls breathing in mice. *J. Clin. Invest.* 2010; 120:4118–4128.
- McCrimmon DR, Speck DF, Feldman JL. Role of the ventrolateral region of the nucleus of the tractus solitarius in processing respiratory afferent input from vagus and superior laryngeal nerves. *Exp. Brain Res.* 1987; 67:449–459. [PubMed: 3653307]
- Meyer G, Kirsch J, Betz H, Langosch D. Identification of a gephyrin binding motif on the glycine receptor beta subunit. *Neuron.* 1995; 15:563–572. [PubMed: 7546736]
- Miyazaki M, Tanaka I, Ezure K. Excitatory and inhibitory synaptic inputs shape the discharge pattern of pump neurons of the nucleus tractus solitarii in the rat. *Exp. Brain Res.* 1999; 129:191–200. [PubMed: 10591893]
- Morgado-Valle C, Baca SM, Feldman JL. Glycinergic pacemaker neurons in preBötzing complex of neonatal mouse. *J. Neurosci.* 2010; 30:3634–3639. [PubMed: 20219997]
- Nikolic Z, Laube B, Weber RG, Lichter P, Kioschis P, Poustka A, Mulhardt C, Becker CM. The human glycine receptor subunit  $\alpha$ 3. Glra3 gene structure, chromosomal localization, and functional characterization of alternative transcripts. *J. Biol. Chem.* 1998; 273:19708–19714. [PubMed: 9677400]
- Owens DF, Boyce LH, David MBE, Kriegstein AR. Excitatory GABA responses in embryonic and neonatal cortical slices demonstrated by gramicidin perforated-patch recordings and calcium imaging. *J. Neurosci.* 1996; 16:6414–6423. [PubMed: 8815920]
- Paton JF, Richter DW. Role of fast inhibitory synaptic mechanisms in respiratory rhythm generation in the maturing mouse. *J. Physiol.* 1995; 484:505–521. [PubMed: 7602541]
- Paxinos, G.; Watson, C. *The Rat Brain Atlas*. Academic Press; San Diego: 1986.
- Rekling JC, Feldman JL. Pre-Bötzing complex and pacemaker neurons: hypothesized site and kernel for respiratory rhythm generation. *Annu. Rev. Physiol.* 1998; 60:385–405. [PubMed: 9558470]
- Ren J, Greer JJ. Modulation of respiratory rhythmogenesis by chloride-mediated conductances during the perinatal period. *J. Neurosci.* 2006; 26:3721–3730. [PubMed: 16597726]

- Saul B, Schmieden V, Kling C, Mulhardt C, Gass P, Kuhse J, Becker CM. Point mutation of glycine receptor alpha 1 subunit in the spasmodic mouse affects agonist responses. *FEBS Lett.* 1994; 350:71–76. [PubMed: 8062927]
- Schmid K, Bohmer G, Gebauer K. Glycine receptor-mediated fast synaptic inhibition in the brainstem respiratory system. *Respir. Physiol.* 1991; 84:351–361. [PubMed: 1656503]
- Shao XM, Feldman JL. Respiratory rhythm generation and synaptic inhibition of expiratory neurons in pre-Bötzinger complex: differential roles of glycinergic and GABAergic neural transmission. *J. Neurophysiol.* 1997; 77:1853–1860. [PubMed: 9114241]
- Shevtsova NA, Manzke T, Molkov YI, Bischoff A, Smith JC, Rybak IA, Richter DW. Computational modelling of 5-HT receptor-mediated reorganization of the brainstem respiratory network. *Eur. J. Neurosci.* 2011; 34:1276–1291. [PubMed: 21899601]
- Singer JH, Talley EM, Bayliss DA, Berger AJ. Development of glycinergic synaptic transmission to rat brain stem motoneurons. *J. Neurophysiol.* 1998; 80:2608–2620. [PubMed: 9819267]
- Smith JC, Morrison DE, Ellenberger HH, Otto MR, Feldman JL. Brainstem projections to the major respiratory neuron populations in the medulla of the cat. *J. Comp. Neurol.* 1989; 281:69–96. [PubMed: 2466879]
- Smith JC, Ellenberger HH, Ballanyi K, Richter DW, Feldman JL. Pre-Bötzinger complex: a brain stem region that may generate respiratory rhythm in mammals. *Science.* 1991; 254:726–729. [PubMed: 1683005]
- Smith JC, Butera RJ, Koshiya N, Del Negro C, Wilson CG, Johnson SM. Respiratory rhythm generation in neonatal and adult mammals: the hybrid pacemaker-network model. *Respir. Physiol.* 2000; 122:131–147. [PubMed: 10967340]
- Smith JC, Abdala AP, Borgmann A, Rybak IA, Paton JF. Brainstem respiratory networks: building blocks and microcircuits. *Trends Neurosci.* 2013; 36:152–162. [PubMed: 23254296]
- Subramanian HH, Chow CM, Balnave RJ. Identification of different types of respiratory neurons in the dorsal brainstem nucleus tractus solitarius of the rat. *Brain Res.* 2007; 1141:119–132. [PubMed: 17291467]
- Wardle RA, Poo MM. Brain-derived neurotrophic factor modulation of GABAergic synapses by postsynaptic regulation of chloride transport. *J. Neurosci.* 2003; 23:8722–8732. [PubMed: 14507972]
- Watanabe E, Akagi H. Distribution patterns of mRNAs encoding glycine receptor channels in the developing rat spinal cord. *Neurosci. Res.* 1995; 23:377–382. [PubMed: 8602277]
- Weiss J, O'Sullivan GA, Heinze L, Chen HX, Betz H, Wässle H. Glycinergic input of small-field amacrine cells in the retinas of wildtype and glycine receptor deficient mice. *Mol. Cell Neurosci.* 2008; 37:40–55. [PubMed: 17920294]
- Weltzien F, Puller C, O'Sullivan GA, Paarmann I, Betz H. Distribution of the glycine receptor  $\alpha$ -subunit in the mouse CNS as revealed by a novel monoclonal antibody. *J. Comp. Neurol.* 2012; 520:3962–3981. [PubMed: 22592841]
- Wong-Riley MTT, Liu Q. Neurochemical development of brain stem nuclei involved in the control of respiration. *Respir. Physiol. Neurobiol.* 2005; 149:83–98. [PubMed: 16203213]
- Wong-Riley MTT, Liu Q. Neurochemical and physiological correlates of a critical period of respiratory development in the rat. *Respir. Physiol. Neurobiol.* 2008; 164:28–37. [PubMed: 18524695]
- Wong-Riley MT, Liu Q, Gao XP. Peripheral-central chemoreceptor interaction and the significance of a critical period in the development of respiratory control. *Respir. Physiol. Neurobiol.* 2013; 185:156–169. [PubMed: 22684042]
- Yokota S, Tsumori T, Oka T, Nakamura S, Yasui Y. GABAergic neurons in the ventrolateral subnucleus of the nucleus tractus solitarius are in contact with Kölliker-Fuse nucleus neurons projecting to the rostral ventral respiratory group and phrenic nucleus in the rat. *Brain Res.* 2008; 1228:113–126. [PubMed: 18634761]
- Young-Pearse TL, Ivic L, Kriegstein AR, Cepko CL. Characterization of mice with targeted deletion of glycine receptor alpha 2. *Mol. Cell Biol.* 2006; 26:5728–5734. [PubMed: 16847326]

### Highlights

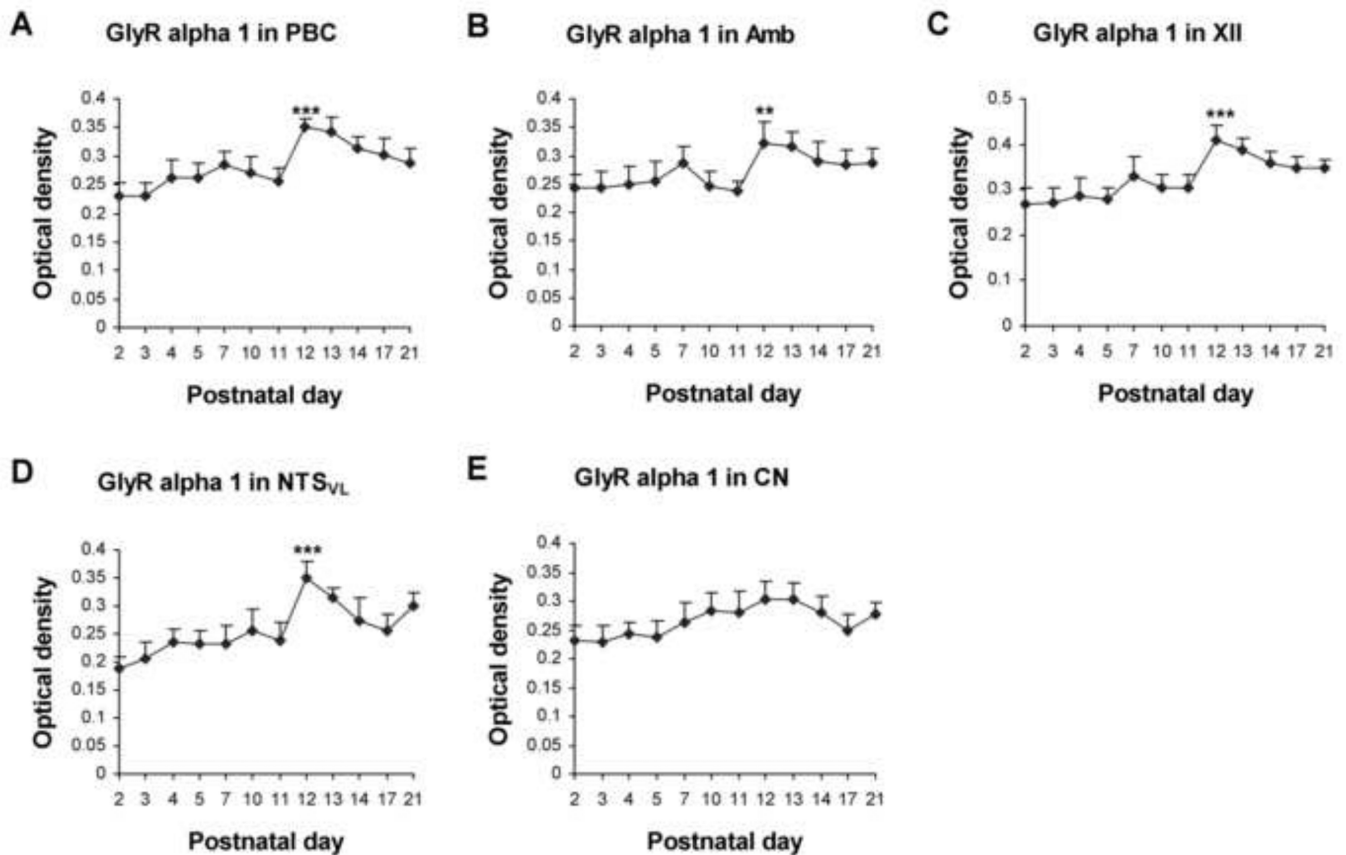
- Four glycine receptor subunits were studied in four respiratory-related nuclear groups.
- Glycine receptor 2 and 3 were relatively high at P2, but declined after 1-1½ weeks.
- Glycine receptor 1 significantly increased at postnatal day (P) 12.
- Glycine receptor rose from P2 to P12, followed by a slight decline thereafter.
- A switch in dominance of glycine receptor subunits at P12 implies enhanced inhibition.



**Figure 1.**

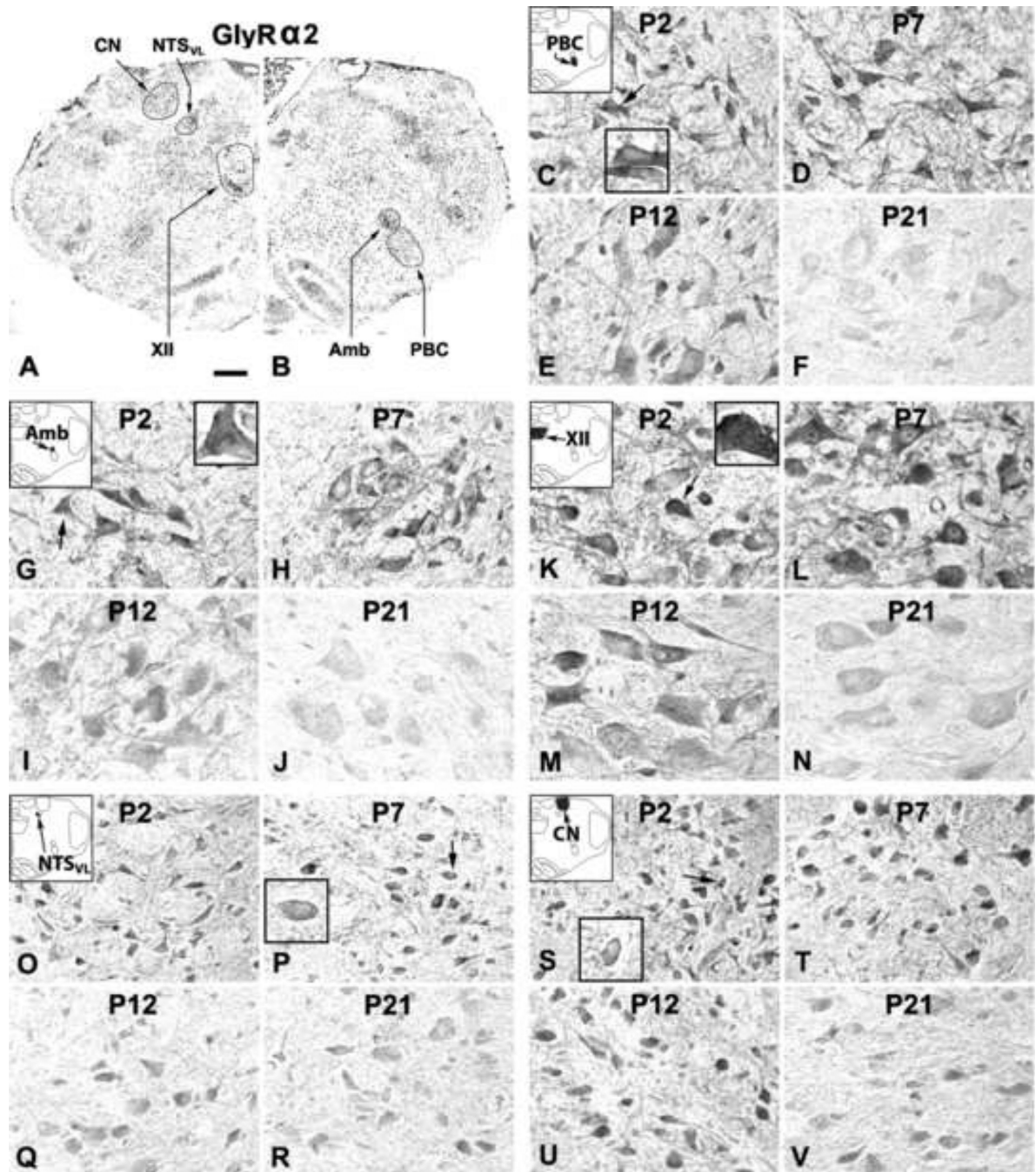
A and B. Low magnification micrograph of rat brain stem section at P7 immuno-reacted for GlyR  $\alpha 1$ . GlyR  $\alpha 1$ -ir neurons and neuropil in the pre-Bötzinger complex (PBC; C-F), nucleus ambiguus (Amb; G-J), hypoglossal nucleus (XII; K-N), ventrolateral subnucleus of the solitary tract nucleus (NTS<sub>VL</sub>; O-R), and cuneate nucleus (CN; S-V) at postnatal days P2, P7, P12, and P21. Diagrammatic locations of each of the five nuclear groups are shown in the upper left corners of C, G, K, O, and S. In the PBC, Amb, XII, and NTS<sub>VL</sub>, GlyR  $\alpha 1$ -ir expression was relatively low at P2, increased slightly at P7, rose significantly at P12, followed by a plateau at P21. Labeling in the neuropil, where neuronal processes and synapses reside, was highest at P12. GlyR  $\alpha 1$  immunoreactivity in the CN increased mildly

from P2 to P12, then stabilized until P21. In all five nuclear groups and at all ages tested, the plasma membrane of labeled neurons also showed immunoreaction product (see arrows and insets in C, F, H, J, K, N, P, R, T, and V). Scale bar: 345  $\mu\text{m}$  for A and B; 20  $\mu\text{m}$  for the rest (6.66  $\mu\text{m}$  for small insets).



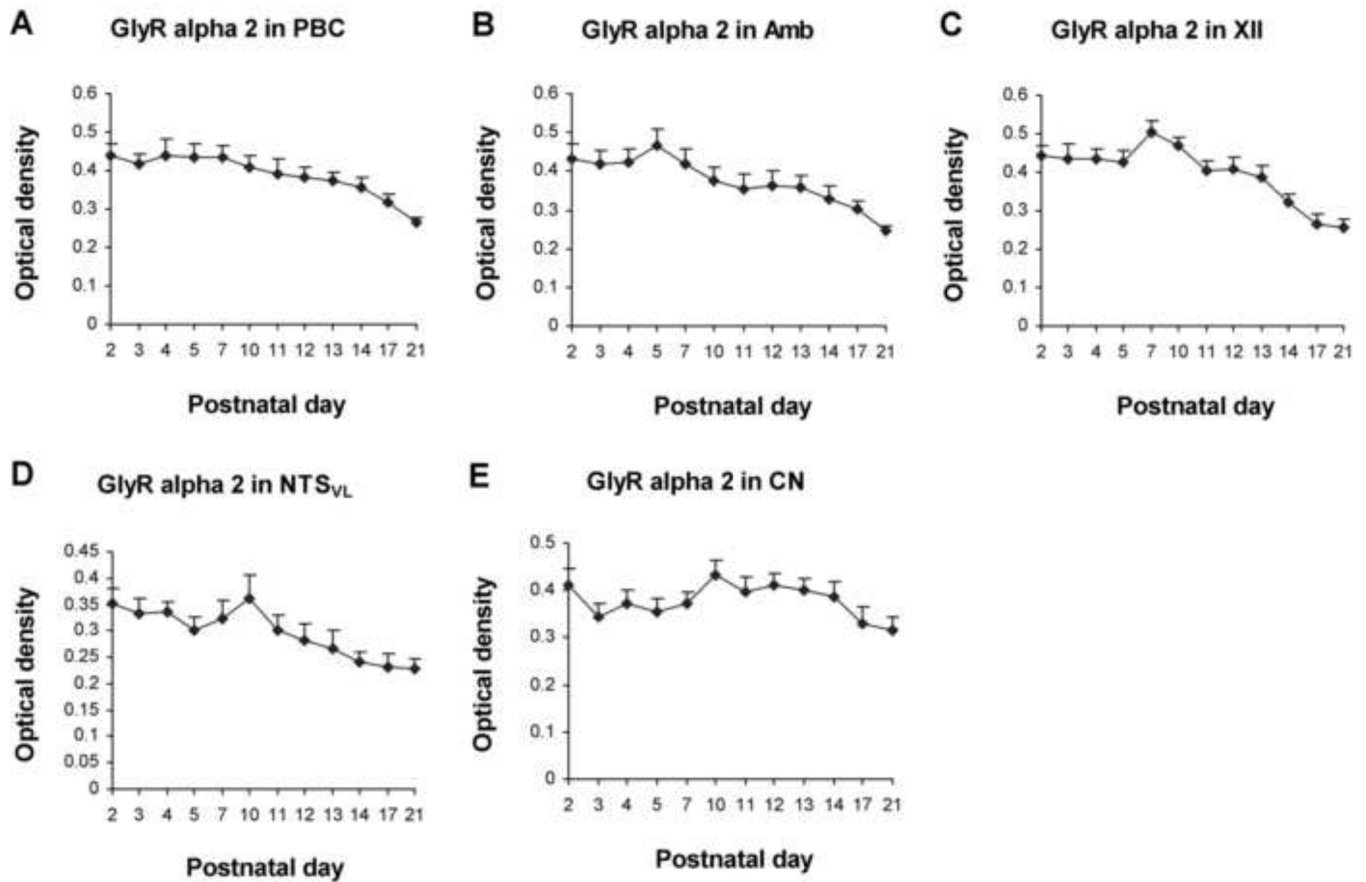
**Figure 2.**

Optical densitometric measurements of immunoreaction product for GlyR  $\alpha$  1 in individual neurons of the PBC (A), Amb (B), XII (C), NTS<sub>VL</sub> (D), and CN (E) from P2 to P21. Data points were presented as mean  $\pm$  SEM. In the first four nuclear groups, GlyR  $\alpha$  1-ir was lowest at P2, increased slightly until P7-10, then rose significantly at P12, followed by either a gradual decline or a plateau until P21. The expression in the CN also increased slightly from P2 to P12-13, but there was not a significant rise at P12. ANOVA yielded significant differences in the expression of GlyR  $\alpha$  1-ir among the ages in the PBC, Amb, XII, and NTS<sub>VL</sub> ( $P < 0.01$ ; not shown), but not in the CN. Tukey's Studentized tests that compared one age group with its immediately adjacent younger age group showed significance only at P12. \*\*,  $P < 0.01$ ; \*\*\*,  $P < 0.001$ .



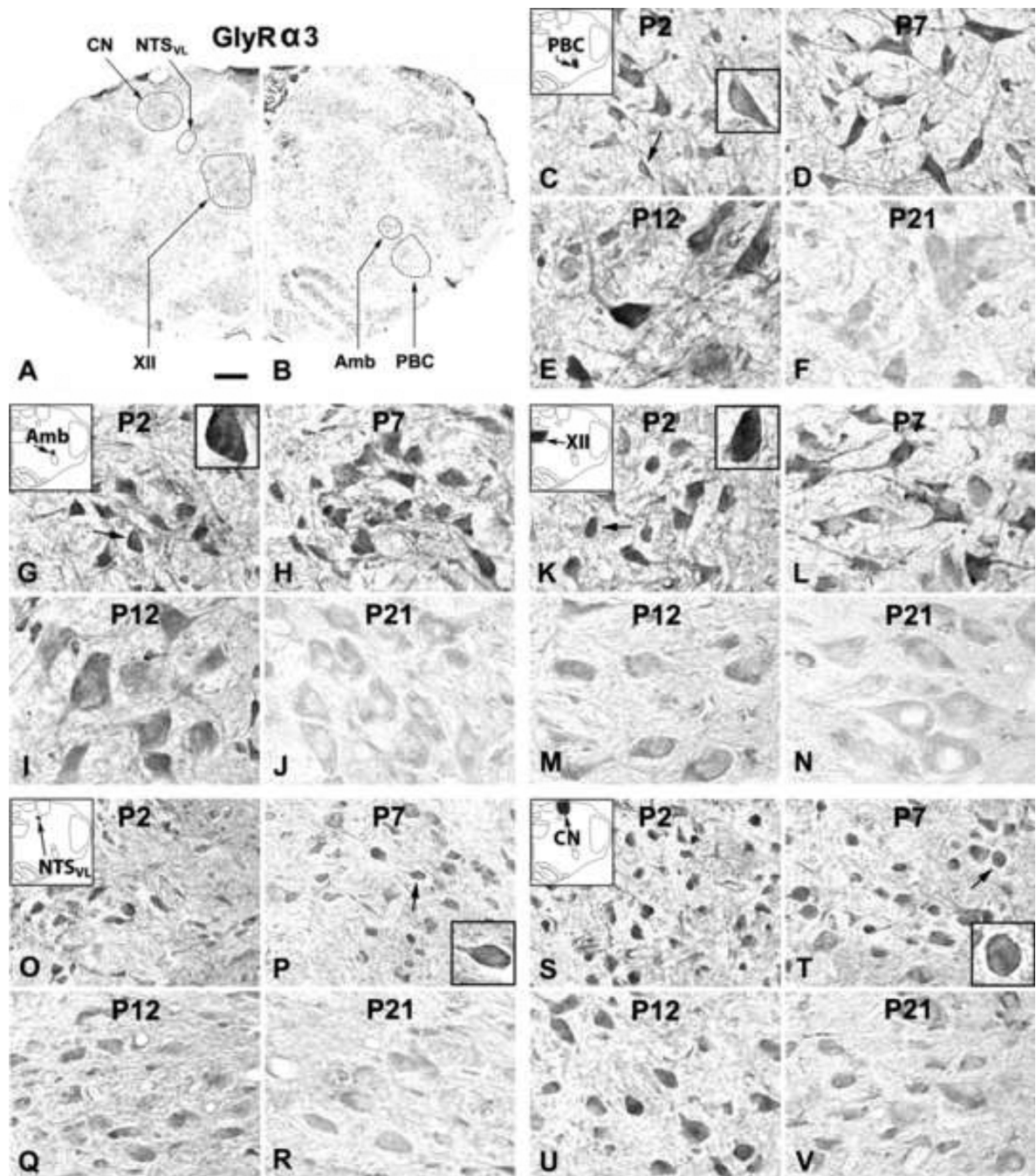
**Figure 3.**

A and B. Low magnification micrograph of rat brain stem section at P7 immuno-reacted for GlyR  $\alpha 2$ . GlyR  $\alpha 2$ -ir neurons and neuropil in the PBC (C-F), Amb (G-J), XII (K-N), NTS<sub>VL</sub> (O-R), and CN (S-V) at P2, P7, P12, and P21. In the first four nuclear groups, GlyR  $\alpha 2$ -ir expression was highest at P2 and P7, slightly reduced at P12, and further reduced at P21. The pattern in the CN was more constant from P2 to P21. The intensity of neuropil labeling in all nuclear groups was similar to those of neuronal cell bodies. Plasma membrane labeling was observable at P2, P7, and P12 (see arrows and insets in C, G, K, P, and S), but was not clearly detectable at P21. Scale bar: 345  $\mu$ m for A and B; 20  $\mu$ m for the rest (6.66  $\mu$ m for small insets).



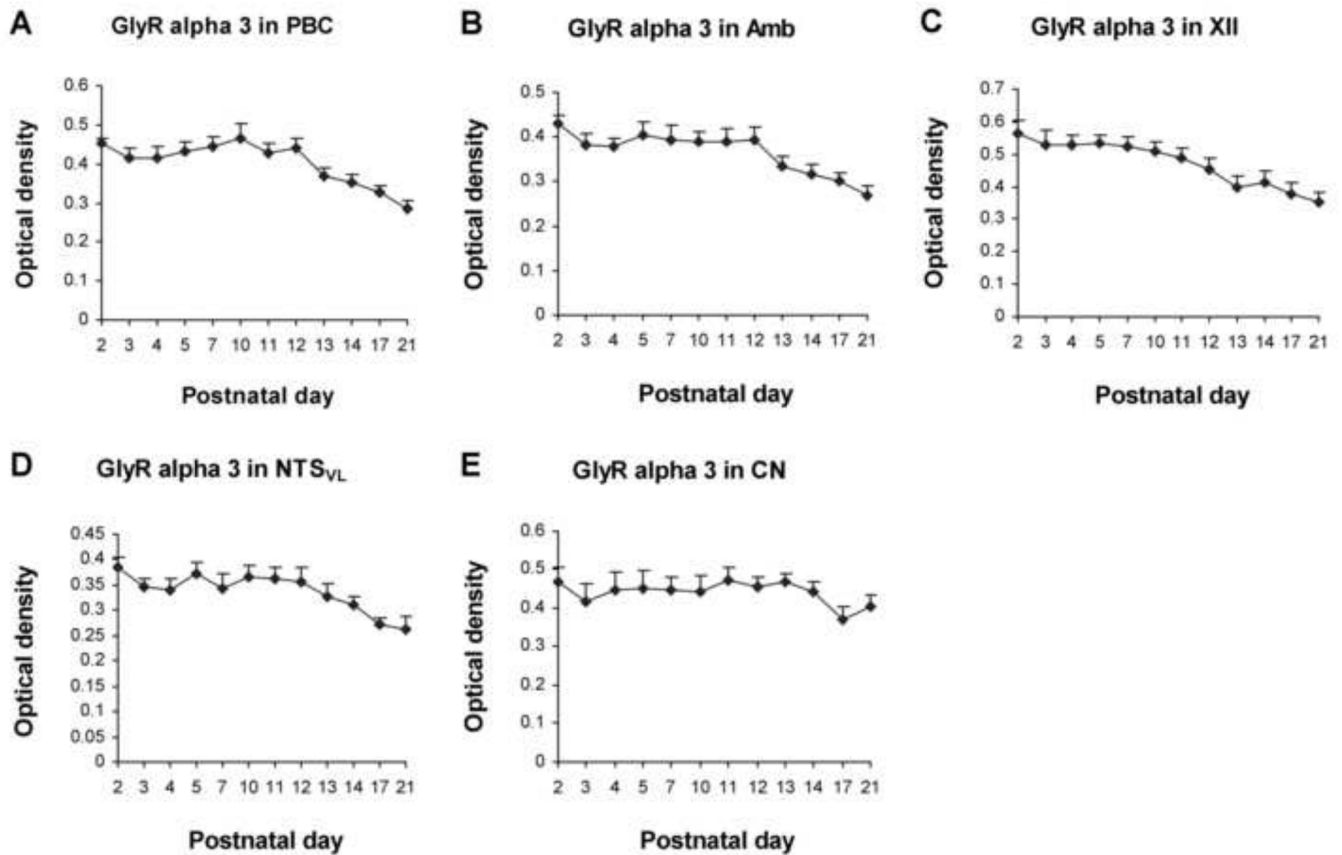
**Figure 4.**

Optical densitometric measurements of immunoreaction product for GlyR  $\alpha$ 2-ir in individual neurons of the PBC (A), Amb (B), XII (C), NTS<sub>VL</sub> (D), and CN (E) from P2 to P21. Data points were presented as mean  $\pm$  SEM. In the first four nuclear groups, GlyR  $\alpha$ 2-ir was relatively high from P2 to P7-10, followed by a gradual decline until P21. Labeling in the CN was relatively stable from P2 to P21, with the lowest value at P21. ANOVA yielded significant differences in the expression of GlyR  $\alpha$ 2-ir among the ages in the first four nuclear groups ( $P < 0.01$ ; not shown), but not in the CN. Tukey's tests did not show significant differences between any two adjacent age groups.



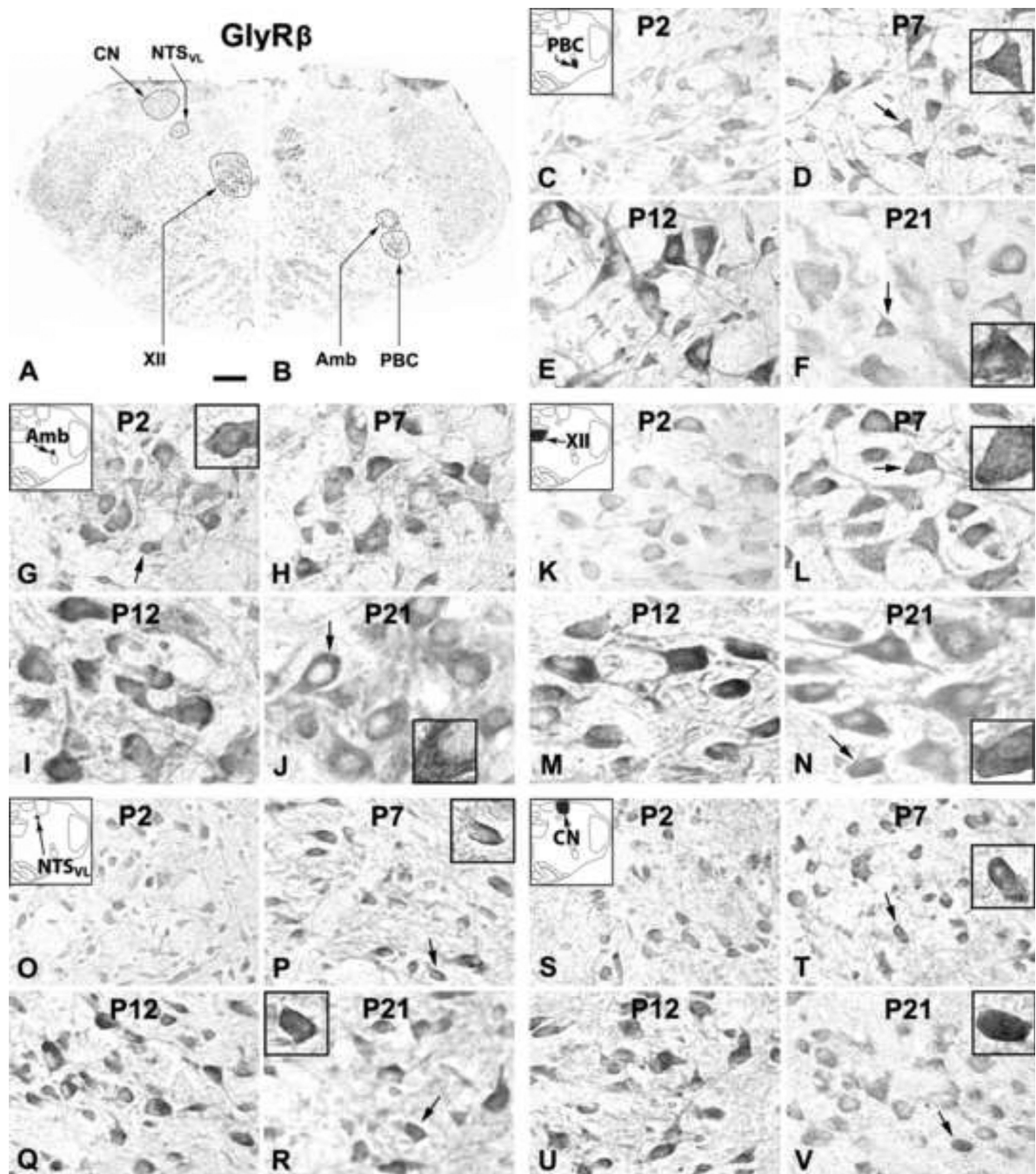
**Figure 5.**

A and B. Low magnification micrograph of rat brain stem section at P7 immuno-reacted for GlyR  $\alpha 3$ . GlyR  $\alpha 3$ -ir neurons and neuropil in the PBC (C-F), Amb (G-J), XII (K-N), NTS<sub>VL</sub> (O-R), and CN (S-V) at P2, P7, P12, and P21. In the first four nuclear groups, GlyR  $\alpha 3$ -ir expression was highest at P2, P7, and P12, but lowest at P21. The expression in the CN was more constant from P2 to P21. The neuropil labeling was relatively constant at P2, P7, and P12, but was reduced at P21. The plasma membrane showed immunoreactions product at P2, P7, and P12 (see arrows and insets in C, G, K, P, and T), but was much fainter at P21. Scale bar: 345  $\mu\text{m}$  for A and B; 20  $\mu\text{m}$  for the rest (6.66  $\mu\text{m}$  for small insets).



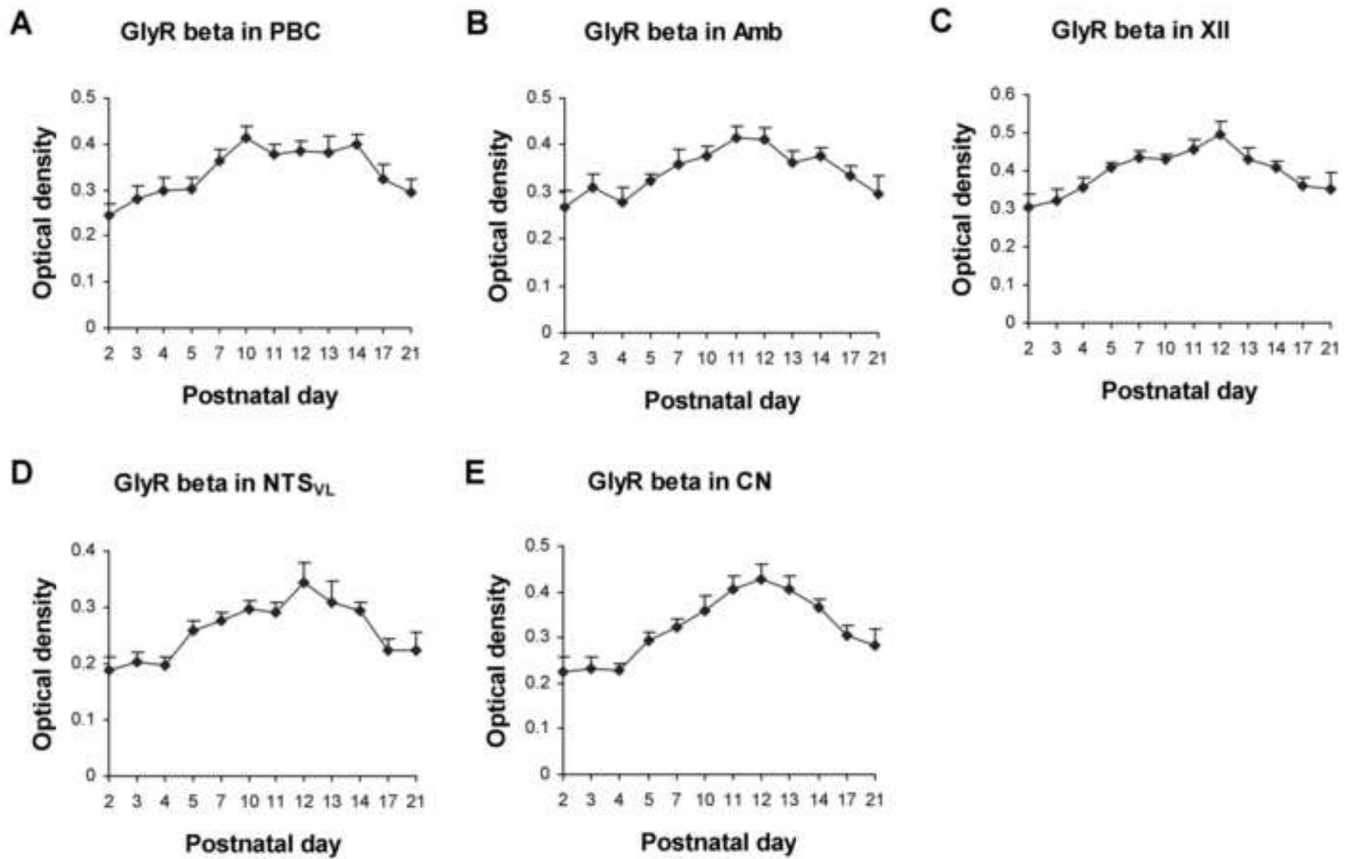
**Figure 6.**

Optical densitometric measurements of immunoreaction product for GlyR  $\alpha$ 3-ir in individual neurons of the PBC (A), Amb (B), XII (C), NTS<sub>VL</sub> (D), and CN (E) from P2 to P21. Data points were presented as mean  $\pm$  SEM. In the first four nuclear groups, GlyR  $\alpha$ 3-ir was relatively high from P2 to P10-12, then declined gradually until P21. The expression in the CN was relatively constant from P2 to P21. ANOVA yielded significant differences in the expression of GlyR  $\alpha$ 3-ir among the ages in the first four nuclear groups ( $P < 0.01$ ; not shown), but Tukey's test did not show significant differences between any two adjacent age groups.



**Figure 7.**

A and B. Low magnification micrograph of rat brain stem section at P7 immuno-reacted for GlyR . GlyR -ir neurons and neuropil in the PBC (C-F), Amb (G-J), XII (K-N), NTS<sub>vL</sub> (O-R), and CN (S-V) at P2, P7, P12, and P21. In all five nuclear groups, the expression was relatively low at P2, increased at P7 and peaked at P12, followed by a slight decline at P21. Labeling intensity in the neuropil was similar to that in neuronal cell bodies. Reaction product on the plasma membrane of labeled neurons was observable at all ages in all five nuclear groups (see arrows and insets in D, F, G, J, L, N, P, R, T, and V). Scale bar: 345 μm for A and B; 20 μm for the rest (6.66 μm for small insets).

**Figure 8.**

Optical densitometric measurements of immunoreaction product for GlyR  $\beta$ -ir in individual neurons of the PBC (A), Amb (B), XII (C), NTS<sub>VL</sub> (D), and CN (E) from P2 to P21. In all five nuclear groups, GlyR  $\beta$ -ir was lowest at P2, increased thereafter to reach a peak around P12, followed by a gradual decline until P21. ANOVA revealed significant differences in the expression of GlyR  $\beta$ -ir among the ages in all five nuclear groups ( $P < 0.01$ ; not shown), but Tukey's test did not yield significant differences between any two adjacent age groups.

**Table 1**

## Primary Antibodies Used

Antigen	Immunogen	Manufacturer, species, type	Catalog number	Dilution used
Glycine receptor 1 subunit (GlyR 1)	Human synthetic GlyR 1 peptide, 24 amino acid between aa 190-239	Santa Cruz Biotech (Santa Cruz, CA), rabbit polyclonal IgG,	sc-133629 (Q-24)	1:150
Glycine receptor 2 subunit (GlyR 2)	Human C-terminus of GlyR 2 (aa 371-420)	Santa Cruz Biotech (Santa Cruz, CA), rabbit polyclonal IgG,	sc-20133 (H-50)	1:400
Glycine receptor 3 subunit (GlyR 3)	15 amino acid synthetic peptide between aa 400-450 of the C-terminus of human GlyR 3	Santa Cruz Biotech (Santa Cruz, CA), goat polyclonal IgG,	sc-17282 (C-15)	1:100
Glycine receptor subunit (GlyR )	20 amino acid synthetic peptide between aa 400-450 of the C-terminus of human GlyR	Santa Cruz Biotech (Santa Cruz, CA), goat polyclonal IgG,	sc-17285 (C-20)	1:300